

N. KOCON¹, J. DZIK^{1*}, D. SZALBOT¹, T. PIKULA²,
M. ADAMCZYK-HABRAJSKA¹, B. WODECKA-DUŚ¹

SYNTHESIS AND DIELECTRIC PROPERTIES OF Nd DOPED Bi₅Ti₃FeO₁₅ CERAMICS

Aurivillius Bi₅Ti₃FeO₁₅ (BTF) and Bi_{5-x}Nd_xTi₃FeO₁₅ (BNTF) ceramics were successfully synthesized by a simple solid state reaction method. Ceramics were prepared from simple oxide powders Bi₂O₃, TiO₂, Nd₂O₃ and Fe₂O₃. The microstructure, structure, chemical composition and dielectric properties of the obtained materials were examined. Dielectric properties were investigated in a wide range of temperatures ($T = 25^{\circ}\text{C}$ - 550°C) and frequencies (20Hz-1MHz).

Keywords: ceramics, sintering, Bi₅Ti₃FeO₁₅, Nd³⁺ doping, microstructure, dielectric properties

1. Introduction

Multiferroic materials that possess simultaneous magnetic and ferroelectric features have attracted interest in recent years because of their special properties, promising applications and especially due to the associated electric and magnetic polarization coupling between the two different orders [1,2]. Important potential applications of these multiferroic materials include electrical transformers, information storage devices such as multi-state non-volatile memories, sensors, phase shifters, amplitude modulators and optical wave devices [3,4]. Multiferroism has been observed in several perovskite-type materials like BiFeO₃, YMnO₃, BiMnO₃ and others [5,6].

Bi₅Ti₃FeO₁₅ (BTF) ceramics can be regarded as a model of the Aurivillius type of single ferroelectromagnetics. The unique interest in this material is caused, among others, by the fact that it is a combination of multiferroic BiFeO₃ and ferroelectric Bi₄Ti₃O₁₂ and can be used for producing advanced materials for information processing and information storage applications [7,8].

The general formula of these compounds is Bi_{m+1}Fe_{m-3}Ti₃O_{3m+3} [9]. These compounds have layered perovskite-like structures, first described by Aurivillius, in which fluorite-like bismuth-oxygen layers of thickness f and composition $\{(\text{Bi}_2\text{O}_2)^{2+}\}_{\infty}$ alternate with (001) perovskite-like slabs of composition $\{(\text{Bi}_{m+1}\text{Fe}_{m-3}\text{Ti}_3\text{O}_{3m+1})^{2-}\}_{\infty}$ and thickness $h = pm$. The values of f and h are related to the c cell parameter by $f + h = c/2$,

m indicates the number of perovskite-like layers per labs and may take integer or fractional values, and p is the average thickness of perovskite-like layers (Fig. 1). Fractional m value corresponds to mixed-layer structures which contain perovskite slabs of different thicknesses [10].

The purpose of this paper was to fabricate Bi_{5-x}Nd_xTi₃FeO₁₅ for $x = 0$ (BTF), 0.03 (BNTF3), 0.05 (BNTF5), 0.07 (BNTF7) and 0.1 (BNTF10) ceramics by a solid state reaction.

The aim of the was to investigate how Nd³⁺ ions influence on samples of Bi_{5-x}Nd_xTi₃FeO₁₅ ceramics, like their structure, microstructure and dielectric properties.

2. Experiment

The Bi₅Ti₃FeO₁₅ (BTF) and Bi_{5-x}Nd_xTi₃FeO₁₅ (BNTF) ceramics were prepared by the conventional solid state reaction route. Analytical-purity oxides: TiO₂, Fe₂O₃, Bi₂O₃ and Nd₂O₃ were weighed carefully and mixed in stoichiometric proportions in the planetary ball mill for 24 h using the YTZ balls as grinding media in the ethanol solution. Dried and mixed powders, were pressed in pellets ($p = 60$ MPa, $d = 23$ mm) and subsequently calcined in air, at $T = 750^{\circ}\text{C}$ for $t = 10$ h. After calcination the samples were crushed and re-grinded. Finally, the pretreated powders were pressed into small pellets at $p = 30$ MPa ($d = 10$ mm) and sintered in air, at 950°C for 3 h. Fig. 2 presents the flow chart of the BTF and BNTF ceramics preparation.

¹ UNIVERSITY OF SILESIA, INSTITUTE OF MATERIALS SCIENCE, 12 ZYTNA STR., 41-200 SOSNOWIEC, POLAND

² LUBLIN UNIVERSITY OF TECHNOLOGY, INSTITUTE OF ELECTRONICS AND INFORMATION TECHNOLOGY, 38A NADBYSTRZYCKA STR., 20-618 LUBLIN, POLAND

* Corresponding author: jolanta.dzik@us.edu.pl



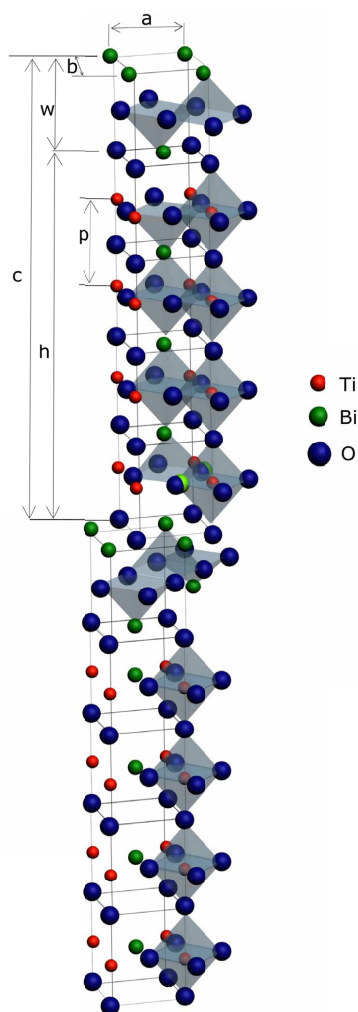


Fig. 1. An elementary cell of Aurivillius structure compound exemplified by $\text{Bi}_4\text{Ti}_3\text{O}_{12}$

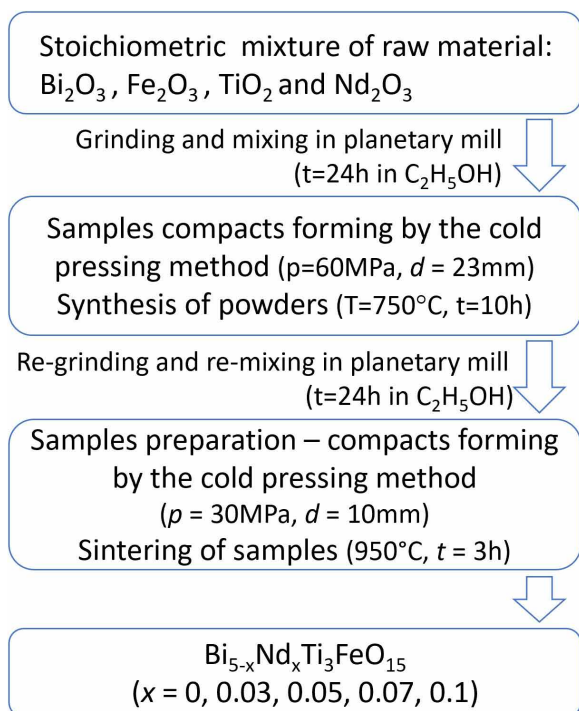


Fig. 2. The flowchart of fabrication process of BTF and BNTF ceramics

The microstructure and chemical composition of the final ceramics were examined with a scanning electron microscope (SEM) JSM - 7100F equipped with an energy dispersive spectrometer (EDS) NORAN Vantage. The microscope was operating at 15 kV acceleration voltage.

The crystal structure of the obtained samples was investigated using Panalytical-Empryan diffractometer with $\text{CuK}\alpha$ radiation. The diffractometer was working in the standard $\Theta - 2\theta$ mode in the 2θ range 10° - 90° and the step $\Delta 2\theta = 0.01^\circ$. The phase and structural analyses of the recorded XRD patterns were performed with an X'Pert HighScore Plus program.

The computerized automatic system based on precision LCR meter Agilent E4980A was used to measure the temperature dependencies of permittivity. Silver electrodes were deposited on BTFO ceramics by firing silver paste at a temperature of $T = 700^\circ\text{C}$ to form parallel plate measuring capacitor.

3. Results and discussion

Fig. 3 shows diffractograms registered for the studied samples after final processing. All the visible peaks were assigned to orthorhombic phase (space group Fmm2) characteristic of $\text{Bi}_5\text{Ti}_3\text{FeO}_{15}$ compound. No additional peaks were detected, thus it may be claimed that the single phase $\text{Bi}_{5-x}\text{Nd}_x\text{Ti}_3\text{FeO}_{15}$ ceramics were obtained. The positions of peaks agree well with the standard pattern indexed by 074037 ICSD card number shown in the bottom panel of Fig. 3.

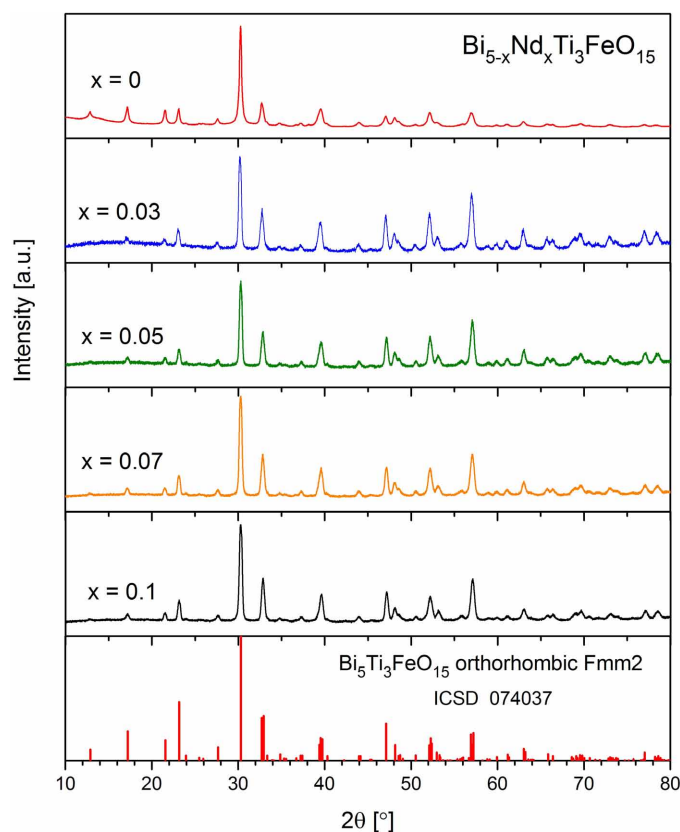


Fig. 3. X-ray diffraction patterns of $\text{Bi}_{5-x}\text{Nd}_x\text{Ti}_3\text{FeO}_{15}$ ceramics

Structural parameters derived from XRD spectra analyses were summarized in Tab. 1. It can be noted that the a and b lattice parameters do not change significantly with the growth of Nd concentration. The c parameter increases from 41.184 Å for $x = 0$ to 41.221 Å for $x = 0.1$ however this is growth by only 0.08 % of the height of the unit cell.

EDS spectrum and SEM micrographs showing the morphology of fracture for BTF ceramics are presented in Fig. 4. The distribution of all elements was investigated with Energy Dispersion X-ray spectrometer (EDS). The presented research was carried out for randomly selected areas. The contents of bismuth, titanium, neodymium and iron elements obtained from EDS analysis were recalculated to the mass of the suitable oxides. The theoretical and experimental content of elements for obtained ceramics is given in Tab. 2. It may be observed that

small deviations from the theoretical composition have occurred but they do not exceed the value of 5%. It is consistent with the resolution of the utilized method of investigation. The analysis of the obtained data proved a homogenous distribution of elements throughout the grains and stoichiometry close to nominal.

SEM micrographs showing morphology of fracture for BNTF ceramics are presented in Fig. 5. All micrographs show a distinct plate-like morphology of BTF, typical for layered compounds belonging to the Aurivillius phases. We can see in the pictures an evident decrease in the grain size of neodymium modified ceramics in comparison with the single phase BTF what is likely related to the fact that rare-earth ions are known to suppress the grain growth in perovskites which can be attributed to their lower diffusivity [11].

TABLE 1

Structural parameters derived from XRD spectra analyses. The uncertainty of a and b lattice parameters is of the order of 0.002 Å while for c it is about 0.007 Å

	Crystal system	Space group	a [Å]	b [Å]	c [Å]	$\alpha = \beta = \gamma$ [°]	V [Å ³]
BTF	Orthorhombic	Fmm2	5.436	5.468	41.184	90	1224.2
BNTF3			5.436	5.462	41.186	90	1222.9
BNTF5			5.435	5.465	41.197	90	1223.6
BNTF7			5.435	5.462	41.211	90	1223.4
BNTF10			5.434	5.456	41.221	90	1222.1

TABLE 2

The theoretical and experimental content of elements (calculation for simple oxide) for BTF and BNTF ceramics

Formula	Oxide content by EDS measurement [%]				Theoretical content of oxides [%]				Content error [%]			
	Bi ₂ O ₃	Fe ₂ O ₃	TiO ₂	Nd ₂ O ₃	Bi ₂ O ₃	Fe ₂ O ₃	TiO ₂	Nd ₂ O ₃	Bi ₂ O ₃	Fe ₂ O ₃	TiO ₂	Nd ₂ O ₃
BTF	7,750	0,560	1,690	—	7,848	0,538	1,614	—	0,786	3,975	4,583	—
BNTF3	7,700	0,565	1,699	0,036	7,811	0,539	1,616	0,034	1,426	4,903	5,140	4,851
BNTF5	7,76	0,560	1,622	0,058	7,787	0,539	1,617	0,057	0,344	3,884	0,287	2,119
BNTF7	7,67	0,567	1,682	0,081	7,762	0,540	1,619	0,080	1,187	5,091	3,906	1,778
BNTF10	7,616	0,565	1,700	0,119	7,725	0,540	1,621	0,114	1,411	4,582	4,880	4,531

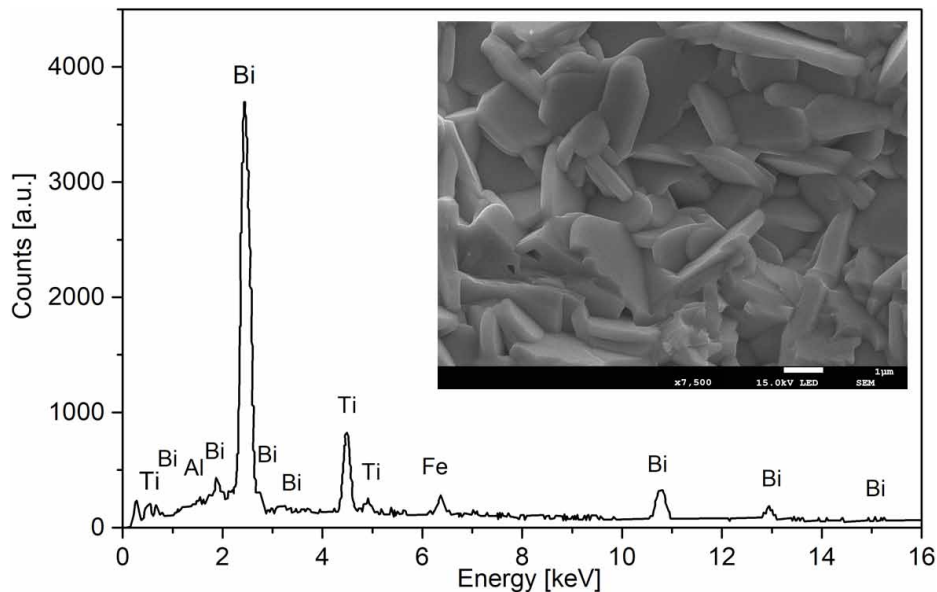


Fig. 4. EDS spectra and SEM micrographs of fracture for BTF

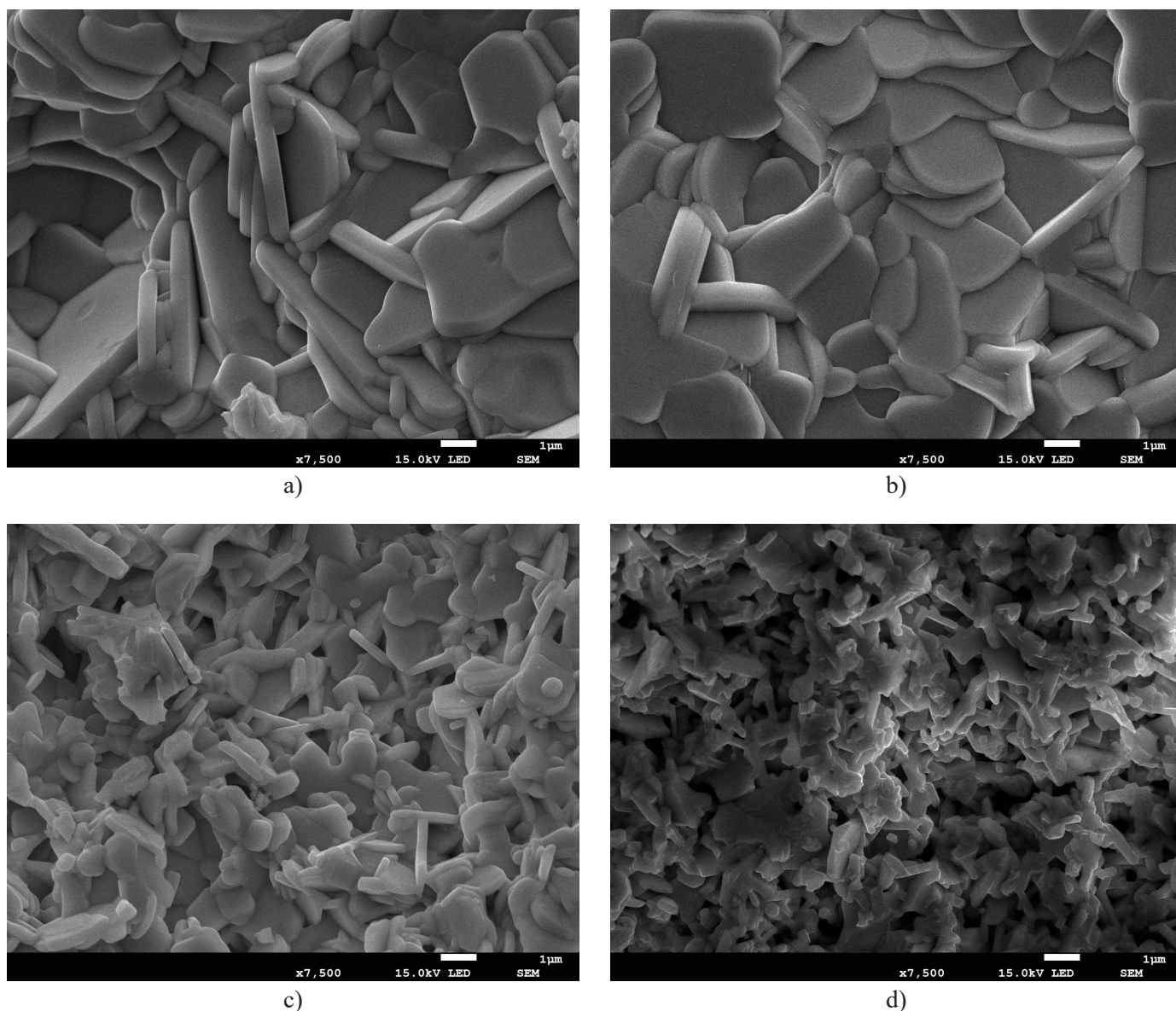


Fig. 5. SEM micrographs of fracture for a) BNTF3; b) BNTF5; c) BNTF7; d) BNTF10 ceramics

The measurements of dielectric permittivity versus temperature were carried out in an electric measuring field at frequencies in the range of 20Hz-1MHz. Fig. 6 shows the frequency dependence of electric permittivity on a temperature for BNTF ceramics. It can be seen that the value of the electrical permittivity of ceramics measured in the frequency range of the measuring field changes with increasing temperature reaching one local maximum and minimum in the temperature range $T = 200-400^{\circ}\text{C}$. As the frequency of the measuring field increases, the $\varepsilon'(T)$ waveforms shift towards higher temperatures, while the absolute permeability values decrease. The curve of the dependence of electric permittivity on temperature shows an increase at different speeds and forms a kind of 'arm' at a temperature of about $T = 450^{\circ}\text{C}$ without reaching the second maximum in the range of the measuring temperature. Such shape of $\varepsilon(T)$ waveforms is characteristic for Aurivillius family described by general formula $\text{Bi}_{5-x}\text{Nd}_x\text{Ti}_3\text{FeO}_{15}$. The origin of the peaks, appearing on $\varepsilon(T)$ dependences at the range of $250^{\circ}\text{C}-270^{\circ}\text{C}$ for BNTF3; BNTF5;

BNTF7 and moves up to 350°C for BNTF10, is not clear. The described maximum should not be connected with the phase transition. This is supported by the following premises: the lack of compliance with the Curie-Weiss law, frequency dependence of maximum value of permittivity, absence of any corresponding anomaly on $\text{tg}\delta(T)$ characteristic at the mentioned range of temperature [12]. The Curie temperature is located at the range of significantly higher temperatures. The Curie temperature for pure $\text{Bi}_5\text{Ti}_3\text{FeO}_{15}$ ceramics is equal 759°C and corresponding to a structural transition from the ferroelectric phase $A21\text{am}$ to paraelectric phase $I4/mmm$ [13]. The same value of Curie temperature has been obtained by other authors [14,15]. In the opinion of the hereby paper the observed broadened peaks corresponds to the space charge polarization, as has been suggested by the authors of following paper [14]. At discussed materials is commonly observed the problem of volatilization of Bi during the calcination process, which leads to the occurrence of Bi vacancies (V''_{Bi}) accompanied by oxygen vacancies (V''_{O}).

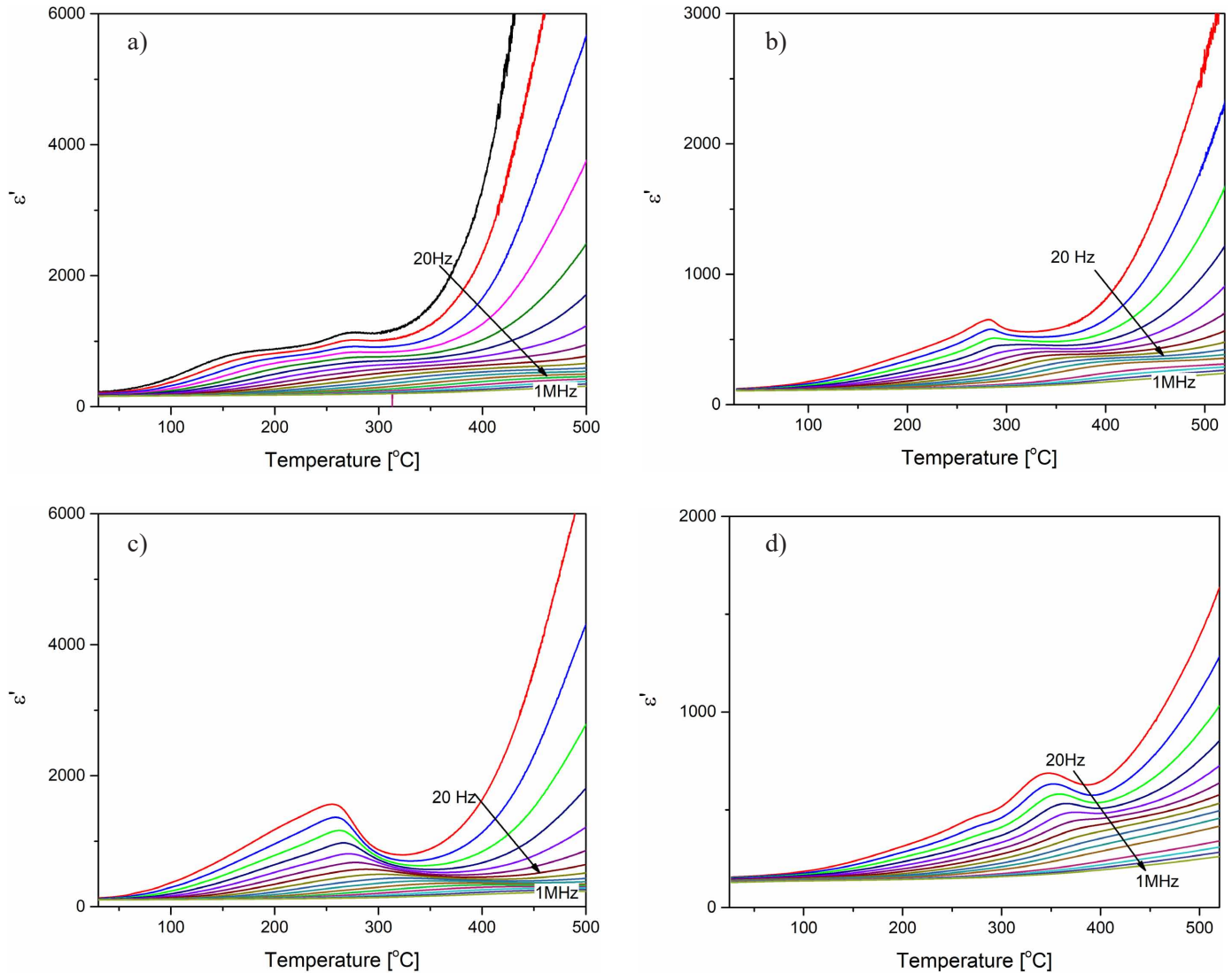


Fig. 6. Temperature dependences of dielectric permittivity for several frequencies chosen for a) BNTF3; b) BNTF5; c) BNTF7; d) BNTF10 ceramics

Fig. 7 shows the frequency dependence of the tangent of the dielectric loss angle on the temperature for BNTF5 and BNTF10 ceramics. The dependence of dielectric loss angle values on the temperature $\text{tg}\delta(T)$ shows a sharp increase with increasing temperature. The $\text{tg}\delta(T)$ curves move towards a higher temperature with an increase in the frequency of the measurement field which indicates a reduction in dielectric losses.

The results of measurements of the dependence of electric permittivity and the tangent of the dielectric loss angle on the temperature for ceramic compounds of the BTFO composition allow to state that ceramics are generally characterized by high dielectric losses of conductivity. The dependence of electric permeability on temperature shows the presence of a wide maximum characteristic for materials with ionic disorder and having relaxation properties.

In order to confirm our assumption concerned the origin of frequency dispersion of dielectric permittivity, measurements of electric conductivity as a function of temperature were carried out at a wide range of temperature. The obtained results are presented in Fig. 8 in the form of the dependence of $\ln\sigma$ vs.

inverse of temperature. At high temperatures all presented dependencies are a constant function of temperature, however, along with the lowering of temperature, the discussed relationships become a linear function of temperature and the process of conductivity assume a clearly activating character. Based on the Arrivilius law:

$$\sigma = \sigma_0 \exp\left(\frac{E_a}{kT}\right)$$

where E_a is the activation energy, σ_0 is specific resistivity at an infinite temperature, the activation energy was calculated and presented in Fig. 8 for all presented dependencies. The low values of E_a may surprise reader at first. However, after a deeper suggestion that such small values may indicate that the conduction might be attributed to the movements of electrons resulting from defects. The data received from literature point out on two kinds of conducting electrons mainly contribute to the low temperature conduction in the investigated materials. The first ones are created by the oxygen vacancy ionization, which main origin is connected with bismuth volatilization at high temperature

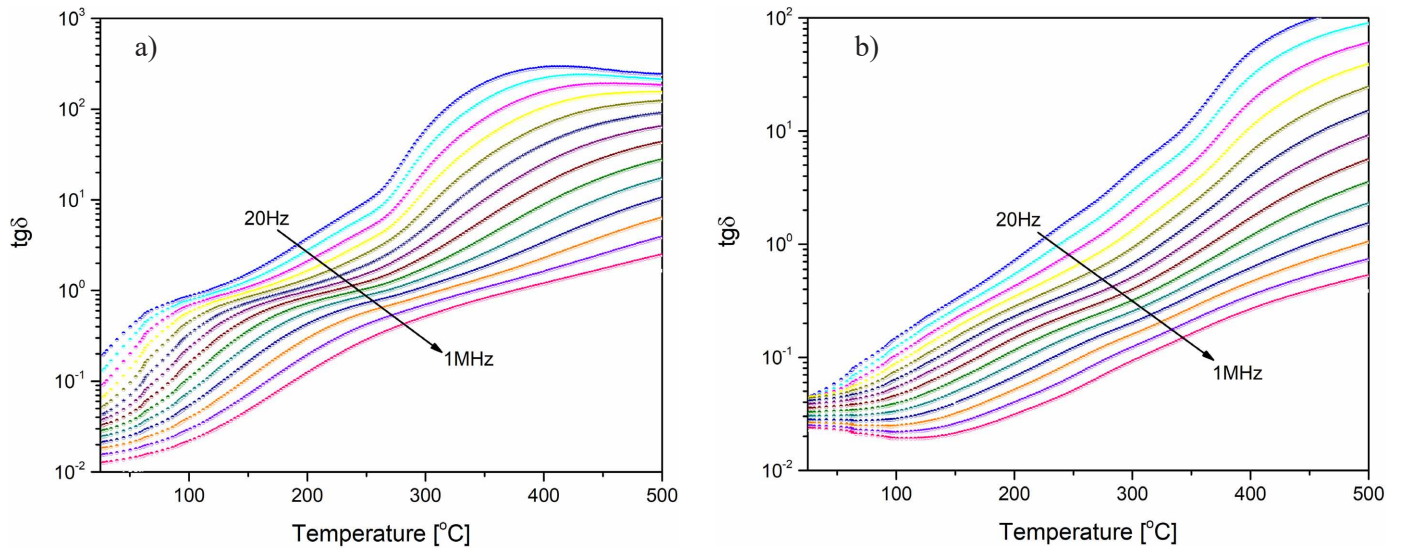


Fig. 7. Temperature dependence of loss tangent for a) BNTF5 and b) BNTF10

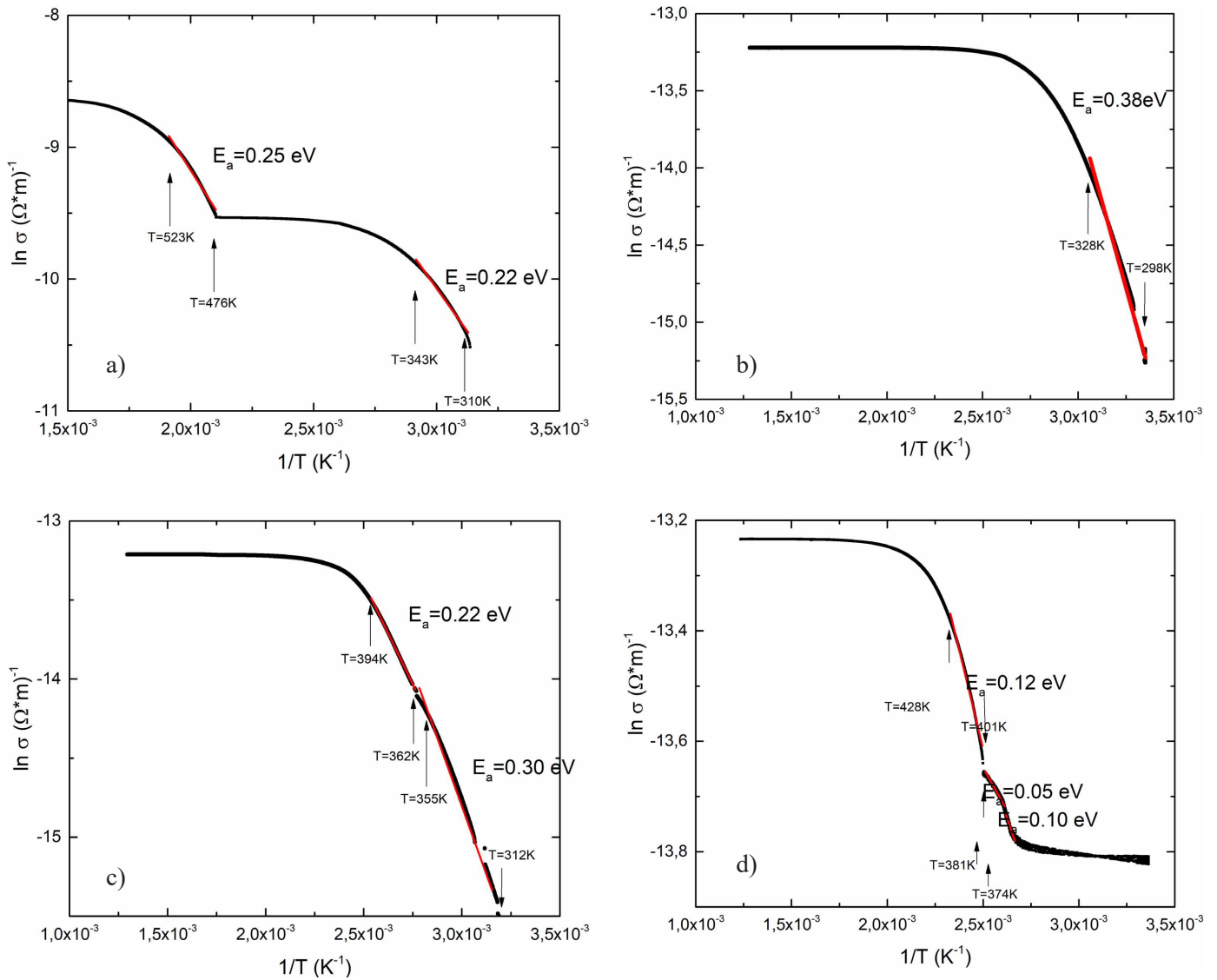


Fig. 8. The natural logarithm of electric conductivity vs inverse temperature for a) BNTF3; b) BNTF5; c) BNTF7; d) BNTF10 ceramics

[16,17]. The second ones are connected with the Fe^{2+} and Fe^{3+} valence fluctuations [18, 19], i.e., $\text{Fe}^{3+} + e' \leftrightarrow \text{Fe}^{2+}$.

4. Conclusions

The $\text{Bi}_5\text{Ti}_3\text{FeO}_{15}$ and $\text{Bi}_{5-x}\text{Nd}_x\text{Ti}_3\text{FeO}_{15}$ ceramic powder was synthesized by the mixed oxide method from the stoichiometric mixture of oxides, viz Bi_2O_3 , Fe_2O_3 , TiO_2 and Nd_2O_3 . All the visible peaks were assigned to the orthorhombic phase (space group Fmm2) characteristic of $\text{Bi}_5\text{Ti}_3\text{FeO}_{15}$ compound. It can be noted that neodymium concentration has significant influence on the grain growth. The increasing the concentration of dopant causes the grain size to decrease. The obtained materials were the single phase and homogeneous samples. Measurements of dielectric permittivity as a function of temperature have shown that as the frequency of the measuring field increases, the $\epsilon(T)$ waveform shifts towards higher temperatures and the absolute permittivity values decrease and the dependence of dielectric loss angle values on temperature $\text{tg}\delta(T)$ shows a sharp increase with an increasing temperature. Measurements of electric conductivity as a function of temperature shown, that all dependencies are a constant function of temperature, but with the lowering of temperature, the discussed relationships become a linear function of temperature and the process of conductivity assume a clearly activating character.

REFERENCES

- [1] H. Zheng, J. Wang, S.E. Lofland, Z. Ma, L.M. Ardabili, T. Zhao, L.S. Riba, S.R. Shinde, S.B. Ogale, F. Bai, D. Viehland, Y. Jia, D.G. Schlom, M. Wuttig, A., Roytued, R. Ramesh, Multiferroic $\text{BaTiO}_3\text{-CoFe}_2\text{O}_4$ nanostructures, *Science* **303**, 661-663 (2004).
- [2] Y. Zhao, Huiqing Fan, G. Liu, Z. Liu, X. Ren, Ferroelectric, piezoelectric properties and magnetoelectric coupling behavior in aurivillius $\text{Bi}_5\text{Ti}_3\text{FeO}_{15}$ multiferroic nanofibers by Electrospinning, *Journal of Alloys and Compounds* **675**, 441 e447 (2016).
- [3] J.D. Bobic, R.M. Katiliute, M. Ivanov, M.M. Vijatovic' Petrovic, N.I. Ilic, A.S. Dzunuzovic, J. Banys, B.D. Stojanovic, Dielectric, ferroelectric and magnetic properties of La doped $\text{Bi}_5\text{Ti}_3\text{FeO}_{15}$ ceramics, *Journal of Materials Science Materials in Electronics* **2** (2015).
- [4] M. Wu, Z. Tian, Songliu Yuan, Zhengbei Huang, Magnetic and optical properties of the Aurivillius phase $\text{Bi}_5\text{Ti}_3\text{FeO}_{15}$, *Materials Letters* **68**, 190-192 (2012).
- [5] M. Čebelaa, D. Zagoraca, K. Batalovićb, J. Radaković, B. Stojadinovićc, V. Spasojević, R. Hercigonj, BiFeO_3 perovskites: A multidisciplinary approach to multiferroics, *Ceramics International* **43**, 1256-1264 (2017).
- [6] E. Arramel under supervision of Beatriz Noheda, Multiferroic thin films, Taken from *Science magazine* **309**, 391(2005) .
- [7] M.S. Wu, Z.M. Tian, S.L. Yuan, H.N. Duan, Y. Qiu, Dielectric behavior and ac conductivity in Aurivillius $\text{Bi}_4\text{Ti}_3\text{O}_{12}$ doped by antiferromagnetic BiFeO_3 , *Physics Letters A* **376**, 2062-2066 (2012) .
- [8] M. Krzhizhanovskaya, S. Filatov, V. Gusarov, P. Paufler, R. Bubnova, M. Morozov, D. C. Meyer, Aurivillius Phases in the $\text{Bi}_4\text{Ti}_3\text{O}_{12}/\text{BiFeO}_3$ System: Thermal Behaviour and Crystal Structure, *Z. Anorg. Allg. Chem.* **631**, 1603-1608.(2005).
- [9] N.A. Lomanova, M.I. Morozov, V.L. Ugolkov, V.V. Gusarov, Properties of Aurivillius Phases in the $\text{Bi}_4\text{Ti}_3\text{O}_{12}\text{-BiFeO}_3$, *System Inorganic Materials* **42**, 2 189 (2006).
- [10] A. Lisinska -Czekaj, E. Jartych, M. Mazurek, J. Dzik, D. Czekaj, Dielektryczne i magnetyczne właściwości ceramiki multiferroicznej $\text{Bi}_5\text{Ti}_3\text{FeO}_{15}$, *Ceramic Materials* **62**, 2, 126-133 (2010).
- [11] W. Cai, K. LiuRongli, G. Xiaoling, D. Gang, C. Chunlin Fu, Influences of La on Optical and Electric Properties of BiFeO_3 Thin Films, *Advanced Functional Materials*, 171-180 (2017).
- [12] J.D. Bobić, R.M. Katiliute, M. Ivanov, M.M. Vijatović Petrović, N.I. Ilić, A. S. Džunuzović, J. Banys, B.D. Stojanović, Dielectric, ferroelectric and magnetic properties of La doped $\text{Bi}_5\text{Ti}_3\text{FeO}_{15}$ ceramics, *Journal of Materials Science: Materials in Electronics* **3** (2016).
- [13] A. Snedden, Ch.H. Hervoches, P. Lightfoot, Ferroelectric phase transitions in $\text{SrBi}_2\text{Nb}_2\text{O}_9$ and $\text{Bi}_5\text{Ti}_3\text{FeO}_{15}$:A powder neutron diffraction study, *Phys. Rev. B* **67** (2003).
- [14] Z. Huang, Gen-Shui Wang, Yu-Ch. Li, Rui-Hong Liang, F. Cao. Xian-L. Dong, Electrical properties of (Na,Ce) doped $\text{Bi}_5\text{Ti}_3\text{FeO}_{15}$ ceramics, *Physica Status Solidi*, **208** (2003).
- [15] A. Starczewska, G. Dercz, J. Dercz, Dielectric and Structural Properties of $\text{Bi}_5\text{Ti}_3\text{FeO}_{15}$ Ceramics Obtained by Solid-State Reaction Process from Mechanically Activated Precursors, *International Journal of Thermophysics* **32** (2011).
- [16] G.I. Skanavi, I.M. Ksendzov, V.A. Trigubenko, V.G. Prokhvatilov, *Zh. Éksp. Teor. Fiz.* **33** (2), 321 (1957) [*Sov. Phys. JETP* **6**, 250 (1958)].
- [17] I. Burn, S. Neirman, Dielectric properties of donor-doped polycrystalline SrTiO_3 , *Journal of Materials Science* **17** (1982).
- [18] Ch. Ang, Z. Yu, L.E. Cross, Oxygen-vacancy-related low-frequency dielectric relaxation and electrical conduction in Bi:SrTiO_3 , *Physical Review B* **62** (2000).
- [19] A.K. Jonscher, A new understanding of the dielectric relaxation of solids, *Journal of Materials Science* **16** (1981).